Journal of Solution Chemistry, Vol. 26, No. 10, 1997

The Freezing Process in Methanol–, Ethanol–, and Propanol–Water Systems as Revealed by Differential Scanning Calorimetry

K. Takaizumi,[1,*] and T. Wakabayashi[2]

Received April 21, 1997; revised August 11, 1997

Solid–liquid phase diagrams, including metastable phases, have been obtained by differential scanning calorimetry (DSC) for methanol–, ethanol–, and propanol–water systems. The metastable solid phases which are initially formed on cooling were detected for these three systems, in order to analyze the freezing processes and to correlate the formation of the metastable phases with solution structure.

KEY WORDS: Lower alcohol–water systems; phase diagram; inflection point; metastable solid phase; solution structure; supercooled liquid.

1. INTRODUCTION

Studying metastable solid phases which are formed on cooling liquid solutions is important for understanding of solute–solvent interactions, especially in water-soluble organic compound-water systems. Although the lower alcohol–water systems are of particular interest because they are very viscous[1] at low temperatures and provide an opportunity to study metastable solid phases, only a few reports are known to us.[1–8]

In a previous paper,[9] we reported on a differential scanning calorimetry (DSC) study of the freezing process and the solid–liquid phase diagram of the water–ethanol system, focusing attention especially on the relation between solution structure and solid phases that separate from the supercooled liquid.

[1]Department of Applied Biological Chemistry, Faculty of Agriculture, Tohoku University, Kawauchi, Aoba-ku, Sendai 980-77, Japan.
[2]Present address: 7-6-52, Dainohara, Aoba-ku, Sendai 981, Japan.

0095-9782/97/1000-0927$12.50/0 © 1997 Plenum Publishing Corporation

We discussed the physical meaning of the inflection point on the liquidus line of the phase diagram appearing at an ethanol mole fraction X of 0.17. This is a remarkable feature common to solid–liquid phase diagrams for lower alcohol–water systems, and we shall denote the inflection point by X^* in all these systems. We assumed that the liquid structure would change abruptly near X^*; that is, at concentrations lower than X^*, the liquid structure will be such that the clustering of water molecules is favorable for nucleation of ice from the supercooled liquid, while at concentrations above X^*, it is unfavorable.

The present paper reports the liquid–solid phase diagrams, including metastable solid phases, for the water–methanol and water–propanol systems obtained by DSC. The water–ethanol system was also reconsidered and studied more carefully than before. Detection of metastable solid phases that initially formed on cooling and determination of their phase compositions were attempted, in order to analyze the freezing process and to correlate the formation of the metastable phases with the solution structure, as was done previously. It was shown that the first solid separated from the supercooled liquid mixture on cooling is ice if $X < X^*$, but a metastable hydrate if $X > X^*$, in all three systems. The inflection point on each liquidus line therefore was understood as a transition point from a liquid structure for aqueous solution to that for alcohol solution, and X^* corresponds to the composition where maxima are found in heat capacity C_p and apparent molar volume V_ϕ[15] at room temperature. Other than the first separated metastable hydrates, there are many metastable solid phases above X^* which seem to increase with the increase in alkyl chain length of alcohol.

2. EXPERIMENTAL

2.1. Materials and Methods

The methanol (MeOH) and propanol (PrOH) used were both of Infinity Pure Grade, 99.8% from Wako Junyaku Co. Ltd., and were used without further purification. Details of the experimental procedures have been described previously.[9]

2.2. Temperature Scanning Program

Five programs for temperature scanning were applied to obtain both metastable and stable phases. The temperature scanning rates were the same; 1 K-min^{-1} for cooling and 0.7 K-min^{-1} for heating, except for Prog. 4 where scanning was at 0.7 K-min^{-1} for cooling and 0.5 K-min^{-1} for heating. The programs were as follows: Prog. 1 (normal): cooling from 30° to −150°C, holding there for 10 min, then heating to 30°C. Prog. 2 (annealing): cooling to $-160°C$, annealing at 130°C for 2 h followed by heating from $-150°C$, and another one in which annealing is carried out at a temperature about 10° lower than the peritectic point. Prog. 3 (partial): a partial melting program by which the separated alcohol hydrate on cooling is almost completely thawed, leaving ice, then again cooling to $-150°C$, and then heating. Prog. 4 (half): this is for examining the first solid phase separated from a supercooled liquid on cooling; cooling to a temperature where first freezing is completed, and then heating to 30°C. Prog. 5: combination of Prog. 3 and Prog. 2; first Prog. 3 is applied, and then Prog. 2.

2.3. Determination of Melting Points

Two cases are distinguished: the phase transition points for the eutectic and peritectic are the onset of melting and of decomposition, respectively, as shown in Fig. 2. For melting of a solid phase in the presence of the liquid phase except for the peritectic, the temperature where melting just finished, *i.e.*, very close to the temperature of the endothermic peak, was assumed to be the melting point. In principle, some corrections should be made, mainly for the time lag due to the finite rate of thermal conduction; however, at the low scanning rates applied here, such minor corrections could be neglected.

The accuracy of temperature determination is believed to be ± 0.3 K, for alcohol concentrations $X < 0.65$ for all three alcohols, while at higher concentrations, $0.65 < X < X_{\text{eutectic}}$, the uncertainty is greater owing to the very high viscosities of these systems at low temperatures.

2.4. Determination of Solid Phase Composition

The composition of the peritectic compound was determined as follows. The enthalpy of decomposition to ice Ih and a liquid solution of the compound at a near-equilibrium state which was attained by annealing for a few hours at about 10°C below the decomposition point, was measured from the thermogram. The enthalpy per unit mass of alcohol was plotted against the mole fraction of alcohol. We assume that the mole fraction where the enthalpy plot shows a break corresponds to the composition of the peritectic as seen from Fig. 1a. The composition of the metastable peritectic compounds, which were obtainable by applying the normal program, was also estimated from the peak in the plot of the enthalpy of decomposition per unit mass of solution *vs.* mole fraction of alcohol. With this program, equilibrium was not attained (Fig. 1b). This method gave much clearer results in determining the compositions than possible alternatives, such as detection of the mole fraction where the eutectic just vanishes. On the other hand, the composition of other hydrates which melt on heating was assumed to be given by the highest melting point in the plot of melting point *vs.* mole fraction, as shown in the figures.

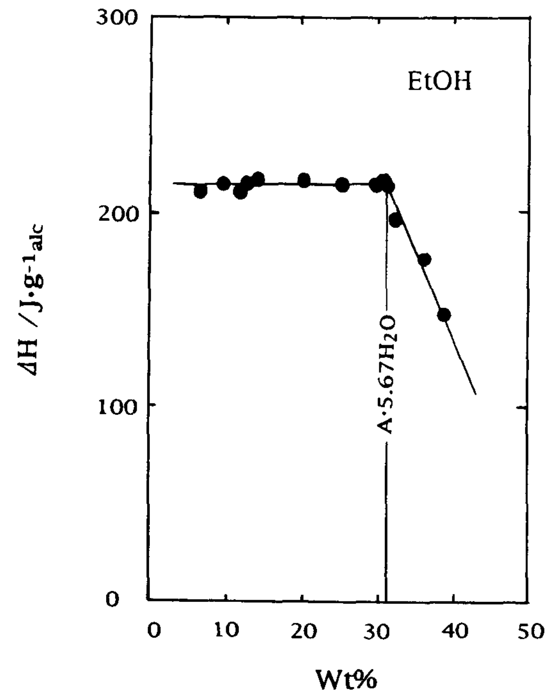

Fig. 1a. Determination of composition of the peritectic stable compound in the ethanol–water system obtained with the annealing program.

3. RESULTS AND DISCUSSION

Typical examples of DSC melting thermograms for methanol–water and propanol–water systems are shown in Fig. 2. Solid–liquid phase diagrams are also shown in Figs. 3a–3c for the three lower alcohol–water systems. Dotted lines in the thermograms show the graphical procedure used to determine the phase transition points. A previously unknown metastable solid phase of methanol was found in the thermograms giving curve b in Fig. 2. The symbols labelling the phase boundaries have the following meanings: A, melting of ice; B, melting of metastable solid other than ice, that is first formed on cooling; D, melting of alcohol hydrate (metastable); E_1, stable eutectic point; E_2, metastable eutectic point; P_1, decomposition of stable peritectic; P_2, decomposition of metastable peritectic. Of the three systems, the water–propanol system was the most difficult to work with. We could not obtain the melting point of pure propanol or the eutectic point, presumably because of the unusually high viscosity of the solution. This incompleteness is, however, not crucial for the present purpose of detecting metastable solid phases. The invariant temperatures, and their corresponding compositions are listed in Tables I and II for all three systems.

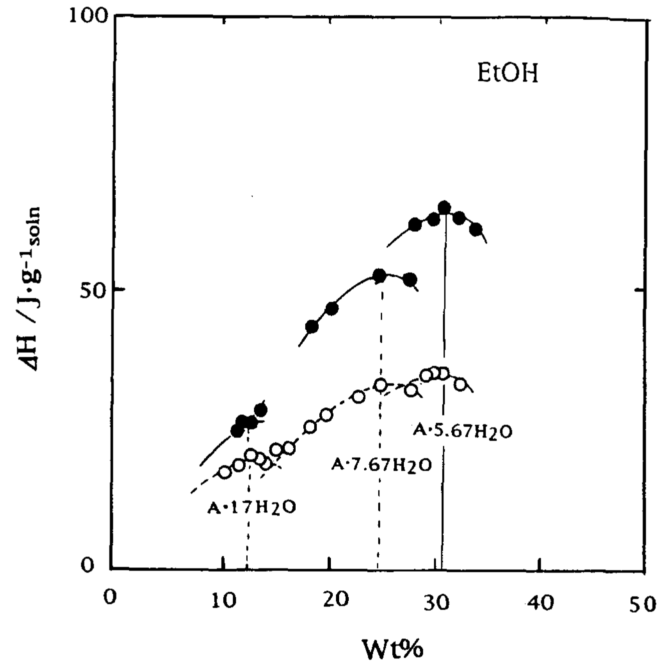

Fig. 1b. Determination of composition of the metastable peritectic (○) obtained by the normal DSC program, and stable peritectic at near-equilibrium (●) obtained by the annealing program.

3.1. Composition of Peritectics

The peritectic hydrates of EtOH and PrOH are listed in Table I. There are some uncertainties in their compositions which were estimated from plots of the enthalpy change per unit mass of solution *vs.* concentration of alcohol, as shown in Fig. 1b for ethanol. There we can distinguish one large peak and two other peaks (or shoulders), corresponding to EtOH·5.67H_2O, EtOH·7.67H_2O, and EtOH·17H_2O, for the highest, second highest, and lowest peak, respectively. Therefore, the results of the present study suggest that both types of clathrates, I and II, are formed with all cages occupied by ethanol guest molecules. Jeffrey and McMullan[10] did X-ray studies of clathrate and clathrate-like hydrates and found that the composition of clathrate I is M·5.75H_2O, M being the guest molecule, when all cages of two types (12 hedra and 14 hedra) are occupied by M, and M·7.67H_2O if only the larger cages are filled. With clathrate II (12 hedra and 16 hedra), the composition is M·17H_2O if only the larger cages are occupied. Thus, the EtOH peritectic may exist as a mixture of clathrate I and clathrate II. Potts and Davidson[11] confirmed the existence of the clathrate II hydrate EtOH·17H_2O below −73.5°C by thermal analysis and dielectric measurements. EtOH·5H_2O with a decomposition temperature of −74°C was reported by Vuillard and

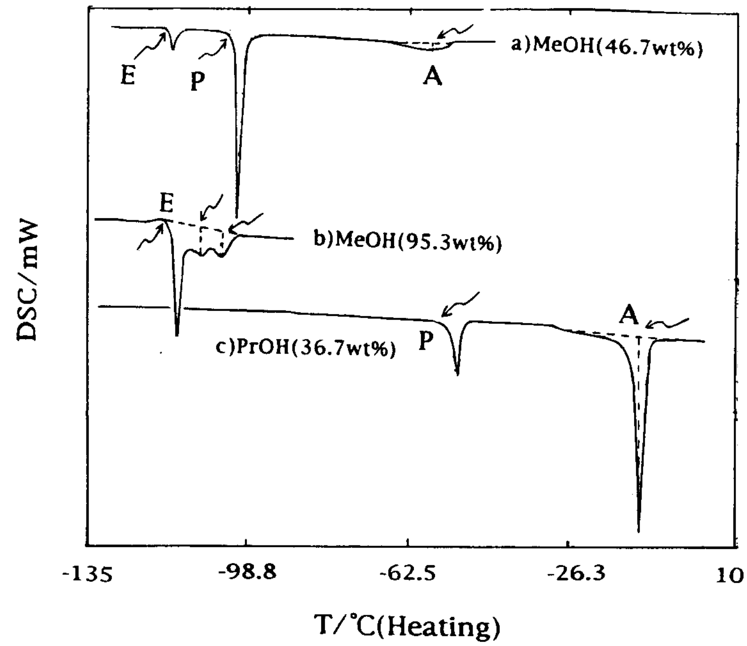

Fig. 2. Typical DSC thermograms: (a) methanol–water (X = 0.33, annealing, at −113°C, 2 hr); (b) methanol–water (X = 0.92, normal program); (c) propanol–water (X = 0.15, annealing, at −70°C, 3 hr).

Satragno[12] from thermal analysis, while Ott *et al.*[1] deduced EtOH·$2H_2O$ by thermal analysis. Calvert and Srivastava[13] reported from X-ray diffraction the formation of two types of ethanol hydrates, clathrate I and "modified clathrate II", the former possibly being stable when a large fraction of its smaller cages are filled with air. Recently Boutron and Kaufmann[2] reached the conclusion from their X-ray diffraction and thermal data that there exist clathrate II hydrate EtOH·$17H_2O$ and, at higher concentrations, another hydrate of composition $46H_2O$ per 6 to 8 EtOH molecules. This is not inconsistent with the present finding of a metastable hydrate. Thus, there remain questions to be addressed in the future.

For PrOH, results similar to those for EtOH were obtained, as can be seen from Table I. From the plot of the enthalpy change, the existence of clathrate I with cages all occupied by propanol molecules and clathrate II of composition PrOH·$17H_2O$, with only the larger cages occupied, are confirmed, despite an expectation that the formation of PrOH·$5.7H_2O$ would be unlikely owing to the difficulty of fitting the propanol molecule into the smaller 12 hedra cage. Apparently there are no reports to compare with the present results.

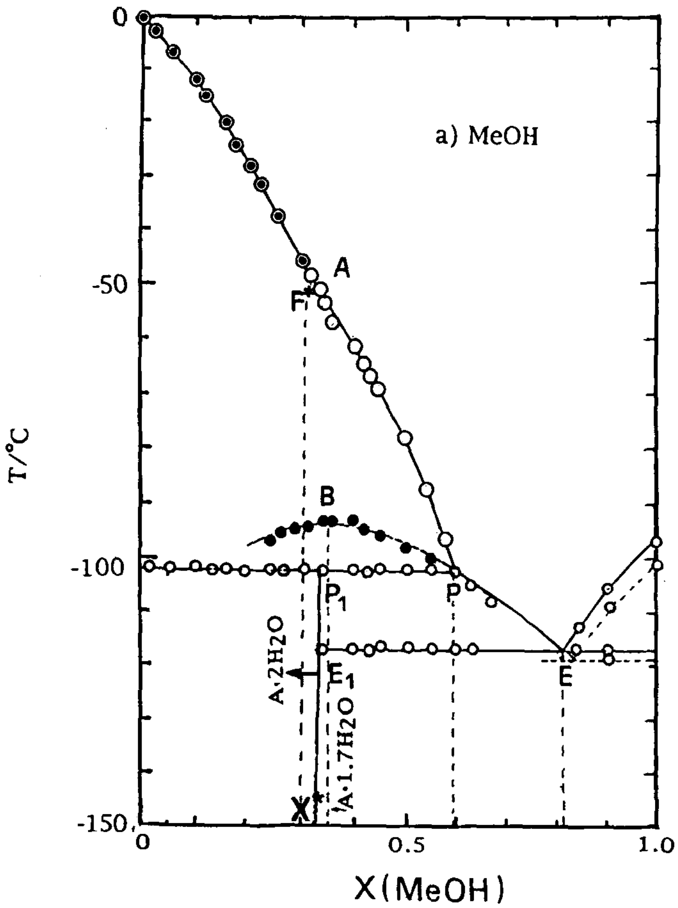

Fig. 3. Solid–liquid phase diagram for lower alcohol–water systems: ○, obtained by normal program; ●, solid first formed from supercooled liquid on cooling; ◒, peritectic compound obtained by melting of solid D leaving ice (by partial melting program); –, equilibrium line; ---, metastable line. A: solid phase first formed from supercooled liquid, ice, B, solid first formed other than ice; D, intermediate compound; P, peritectic; E, eutectic, (a) methanol–water, (b) ethanol–water, (c) propanol–water.

The composition of peritectic methanol hydrate obtained here is $MeOH{\cdot}2H_2O$, which is inconsistent with the monohydrate reported by Ott *et al.*[1] from their phase diagram.

3.2. Freezing Process

The present study systematically revealed the existence of metastable solid phases, which have so far been known only partially, in the middle range of concentration as shown in Figs. 3a–3c.[1,2,9]

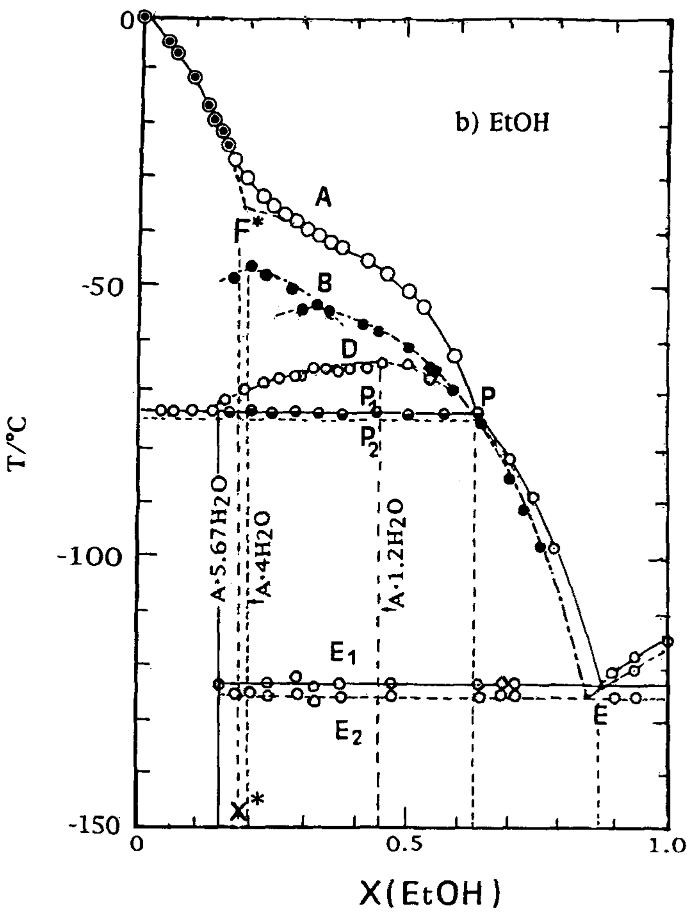

Fig. 3 Continued.

The metastable solid phases begin to appear around X^*, which is the composition for the inflection point on the liquidus line; common to all systems examined: the first separated solid phase from supercooled liquid on cooling is ice Ih in the concentration range below X^*, while at higher concentrations, metastable hydrate B as marked in Figs. 3a–3c appears, though its composition depends on the alcohol and alcohol concentration as shown in Table II. Except for the methanol system, the hydrate B is transformed to another metastable (but kinetically very stable) solid phase D during the temperature decreasing scanning. Thus, to obtain a thermodynamically stable peritectic hydrate, a special temperature scanning program was essential, that is, a partial melting program such that the hydrate D formed would melt leaving ice. The hydration number of hydrate D seems to be 1.2 for both

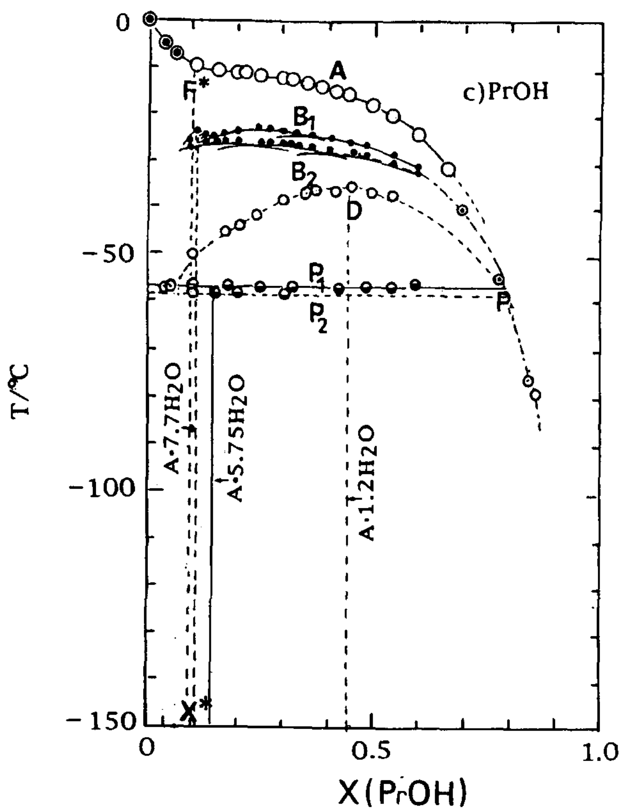

Fig. 3 Continued.

EtOH and PrOH. From the above we can conclude that the peritectic hydrate is formed only by the reaction of ice Ih with the residual liquid solution. In the methanol–water system, the second hydrate D apparently does not exist, and the peritectic hydrate is easily formed without annealing or without applying a partial melting program. This suggests that the formation of the hydrate D is characteristic of the alcohols, such as ethanol and propanol, which form clathrates or clathrate-like hydrates. The lower alcohol–water systems studied here are unusual in the sense that thermodynamically unstable solid phases have higher melting points than the transition points (peritectic points) of the stable solids. The reason for this may be that these metastable solids are prevented from rearrangement to form the thermodynamically stable peritectics by a potential barrier arising from the extraordinarily high viscosity of their solutions at low temperatures.

Table I. Composition of Solid Phases and Invariant Points in Lower Alcohol–Water Systems

		MeOH	EtOH	PrOH
A[a]	Stable	Ice	Ice	Ice
B	Metastable	Solid phase first formed from supercooled liquid on cooling (Table II)		
D	Metastable		*ca* A · $1.2H_2O$[b] -65.0°C	*ca.* A · $1.2H_2O$ -35.2°C
P_1	Stable Peritectic	A · $2H_2O$ -102.5°C	A · $5.67H_2O$ -73.9°C	A · $5.75H_2O$ -53.6°C
P_2	Metastable Peritectic		A · $17H_2O$[c] A · $7.67H_2O$ A · $5.75H_2O$	A · $17H_2O$ A · $7.67H_2O$
E_1	Stable Eutectic	$X = 0.80$ -117.3°C	$X = 0.86$ -124.3°C	Not detected
E_2	Metastable Eutectic	$X = 0.82$ -118.5°C	$X = 0.84$ -125.0°C	Not detected

[a] Symbols in column 1 correspond to those in the figures.
[b] Symbol A in the hydrate formulas denotes the alcohol.
[c] The hydrates are assumed to contain air.

Table II. Composition and Melting Point of the First Solid Formed on Cooling[a]

		MeOH	EtOH	PrOH
B	metastable	A · $1.7H_2O$ -91.3°C	A · $4H_2O$ -47.5°C A · $2H_2O$ -52.5°C	A · $7.7H_2O$ -24.0°C A · $5.7H_2O$ -26.0°C A · $3H_2O$ -23.0°C A · $2H_2O$ -26.3°C A · $1.5H_2O$ -27.5°C

[a] The symbol A in the hydrate formula denotes the alcohol.

3.3. Relation Between Freezing Process and Solution Structure

The results described above are very interesting, taking into account the following:

(1) The coincidence between the composition at the inflection of the liquidus line and the appearance of the first hydrate.

(2) The increasing order in X^*, 0.1 for PrOH $<$ 0.17 for EtOH $<$ 0.3 for MeOH, which is in the same order as the mole fraction of alcohol at

which extrema appear in the partial molar volume and heat capacity of alcohol in solution.[14]

(3) The increasing prominence of the inflection in the order MeOH < EtOH < PrOH parallel to that in the extrema in volume and heat capacity.[14]

These facts strongly suggest the occurrence of some abrupt change in solution structure near these compositions. Thus, the alcohol–water systems can be divided into three concentration regions according to the freezing processes, each of which reflects the solution structure.

3.3.1. Region 1

Water-rich region: alcohol in water as solvent, $X < X^*$. Alkyl groups are completely surrounded by a water layer where water molecules adjacent to alkyl groups will somehow be modified in their orientation and energy in comparison with bulk water (*i.e.*, will undergo hydrophobic hydration). In this situation ice nuclei can form on cooling.

3.3.2. Region 2

Transient region: a narrow range of concentration above X^*. Here, direct contact between alkyl groups begins to occur and a population of small clusters of alcohol molecules increases rapidly with increasing alcohol concentration. In this concentration range, ice and hydrate B can be formed on cooling, and the freezing point depression of ice decreases sharply because contact among alkyl groups results in a decreasing probability for water molecules to interact with alkyl groups. Thus, the inflection on the liquidus line appears. Considering the difference in the number of water molecules required to surround the alkyl groups, X^* should depend on the size of alkyl group, as we find in this study. Our data are inconsistent with the results of Mashimo and Umehara,[15] who concluded that the solution structures change at the same concentration $X = 0.17$ for MeOH, EtOH, and PrOH.

3.3.3. Region 3

Water in alcohol as solvent: $X > X^*$. Further increase in alcohol concentration causes water molecules to interact mainly with hydroxyl groups of the alcohol through hydrogen bonding, and water molecules do not "see" enough water molecules to form ice nuclei on cooling. Here the solid first formed is not ice, but the hydrate B.

Mizuno *et al.*[17–19] made careful NMR and FT-IR measurements on alcohol–water mixtures to determine hydrogen-bonding interactions. As can be seen from their results for the ethanol–water system, the composition dependence of the chemical shift of the water proton and the frequency of the H–O–H bending vibrational band, each show three turning points near X equal to 0.15, 0.65, and 0.85 in the liquid state, which are then interpreted as transition points in solution structure. These points are essentially identical with the discontinuities labelled X^*, P, and E in Fig. 3b, at compositions $X^* = 0.17$, $X_P = 0.63$, and $X_E = 0.86$. The solid first deposited from supercooled liquid on cooling is pure ice (as already discussed) for $0 < X < X^*$; for EtOH hydrates of various compositions depending on $X^* < X < X_P$; *ca.* EtOH·1.2H_2O for $X_P < X < X_E$; and pure ethanol for $X > X_E$. Similar correlations are seen in methanol–water and propanol–water systems.

Recently Takei *et al.*[20] studied dielectric properties of water–EtOH solutions by measuring the resonance frequencies f_R. The plot of f_R and conductivity σ *vs.* mole fraction of EtOH shows a clear break point at $X \approx 0.15$ (close to $X^* = 0.17$), indicating that the structure of a binary solution changes at $X \approx 0.15$; that is, below $X \approx 0.15$ the relative dielectric constant ϵ_r and σ of the solution show perturbations from the properties of pure water, and above $X \approx 0.15$ they are determined largely by the properties of pure alcohol.

There are many discussions concerning the clustering structure of molecules in solution based on various kinds of measurements, especially X-ray and neutron diffraction.[21–25] Mashimo and Umehara[15–16] inferred from dielectric relaxation of ethanol–water mixtures that chainlike clusters of alcohol and water are formed at alcohol concentrations above $X = 0.17$ and, finally, that the chain-like clusters form a network through hydrogen bonding between chains.

With regard to solution structure, we believe that hydration in solution is reflected in the compositions of hydrate B, hydrate D, and the peritectic only indirectly. Thus, we say nothing about the size and shape of ethanol and water clusters in the liquid state at higher concentrations in the present work. We think, however, that chain-like clusters of ethanol will be the basic structures, as in the solid ethanol, and water molecules will be hydrogen-bonded with hydroxyl groups of alcohol molecules at the end of chain-like clusters. The size of clusters will depend on the concentration of alcohol. The present results will obviously have to be confirmed by other methods.

REFERENCES

1. J. B. Ott, J. R. Goates, and B. A. Watte, *J. Chem Thermodyn.* **11**, 739 (1979).
2. P. Boutron and A. Kaufmann, *J. Chem. Phys.* **68**, 5032 (1978).
3. P. Bouton, A. Kaufmann, and N. V. Dang, *Cryobiology* 16, 372 (1979).
4. F. L. Oetting, *J. Phys. Chem.* **67**, 2757 (1963).
5. G. A. Miller and D. K. Carpenter, *J. Chem. Eng. Data.* **9**, 371 (1964).
6. G. Vuillard and M. Sanchez, *Bull. Soc. Chim. Fr.* 1877 (1961).
7. J. C. Rosso and L. Carbonnel, *Comptes rendus.* **Series C**, 1012 (1969).

8. J. C. Rosso and L. Carbonnel, *Comptes rendus.* **Series C**, 4 (1968).
9. K. Takaizumi and T. Wakabayashi, *Cryo-Letters* **16**, 41 (1995).
10. G. A. Jeffrey and R. K. McMullan, *Prog. Inorg. Chem.* **8**, 43 (1967).
11. A. D. Potts and D. W. Davidson, *J. Phys. Chem.* **69**, 996 (1965).
12. G. Vuillard and N. Satragno, *Compt. Rend.* **250**, 3841 (1960).
13. L. D. Calvert and P. Srivastava, *Acta Cryst. Sect.* **A25** S131 (1969).
14. F. Franks and J. E. Desnoyers, *Alcohol–Water Mixtures Revisited*, in *Water Science Reviews*, Vol. 1, F. Franks, *ed.*, pp 171–227, (Cambridge University Press, Cambridge, 1985).
15. S. Mashimo and T. Umehara, *J. Chem. Phys.* **95**, 6257 (1991).
16. S. Mashimo, T. Umehara, S. Kuwabara, and S. Yagihara, *J. Phys. Chem.* **93**, 4963 (1989).
17. K. Mizuno, K. Oda, and A. Okumura, *J. Phys. Chem.* **99**, 3056 (1995).
18. K. Mizuno, Y. Miyashita, and Y. Shindo, *J. Phys. Chem.* **99**, 3225 (1995).
19. K. Mizuno, Y. Kimura, Y. Shindo, in *18th Symposium on Solution Chemistry*, Japan, Kusatsu, 1995.
20. S. Takei, Y. Sugitani, T. Amano, and Y. Nishimoto, *Bunseki Kagaku* **45**, 903 (1996).
21. A. H. Narten and H. A. Levy, *J. Chem. Phys.* **55**, 2263 (1971).
22. A. H. Narten and A. Habenshuss, *J. Chem. Phys.* **80**, 3387 (1984).
23. K. Nishikawa and T. Iijima, *J. Phys. Chem.* **97**, 10824 (1993).
24. N. Nishi, S. Takahashi, M. Matsumoto, A. Tanaka, K. Muraya, T. Takamuku, and T. Yamaguchi, *J. Phys. Chem.* **99**, 462 (1995).
25. M. Matsumoto, N. Nishi, T. Furusawa, M. Saita, T. Takamuku, M. Yamagami, and T. Yamaguchi, *Bull. Chem. Soc. Japan* **68**, 1775 (1995).